

Low resource FPGA-based Time to Digital Converter

Alessandro Balla, Matteo Beretta, Paolo Ciambrone, Maurizio Gatta, Francesco Gonnella, Lorenzo Iafolla[†], Matteo Mascolo, Roberto Messi, Dario Moricciani, Domenico Riondino

Abstract— Time to Digital Converters (TDCs) are very common devices in particles physics experiments. A lot of “off-the-shelf” TDCs can be employed but the necessity of a custom Data acQuisition (DAQ) system makes the TDCs implemented on the Field-Programmable Gate Arrays (FPGAs) desirable. Most of the architectures developed so far are based on the tapped delay lines with precision down to 10 ps [1], obtained with high FPGA resources usage and non-linearity issues to be managed. Often such precision is not necessary; in this case TDC architectures with low resources occupancy are preferable allowing the implementation of data processing systems and of other utilities on the same device. In order to reconstruct $\gamma\gamma$ physics events tagged with High Energy Tagger (HET) in the KLOE-2 (K LOng Experiment 2), we need to measure the Time Of Flight (TOF) of the electrons and positrons from the KLOE-2 Interaction Point (IP) to our tagging stations (11 m apart). The required resolution must be better than the bunch spacing (2.7 ns). We have developed and implemented on a Xilinx Virtex-5 FPGA a 32 channel TDC with a precision of 255 ps and low non-linearity effects along with an embedded data acquisition systems and the interface to the online FARM of KLOE-2.

Index Terms—DAΦNE, DAQ, FPGA, KLOE-2, TDC.

I. INTRODUCTION

TIME to digital converters are largely used in high energy physics and in others fields of science and engineering. Since they are employed with many types of detectors and in many kinds of experiments, it is often necessary to make a trade-off between the most important features: resolution, range, precision and nonlinearities, environment variation effects, dead time, readout speed and customizability of its DAQ, etc. The last point makes the TDCs implemented on the FPGA very attractive; besides nowadays, FPGA-based TDCs reached very good precisions (down to few picoseconds) [1].

Manuscript received June, 2012. This work was supported by the Italian National Institute of Nuclear Physics (INFN).

L. Iafolla was with the National Laboratories of Frascati (LNF) of INFN, via E. Fermi 40, 00044 Frascati (RM), Italy and with the University of Rome “Tor Vergata” – Electronic engineering department (✉e-mail: lorenzo.iafolla@lnf.infn.it).

A. Balla, M. Beretta, P. Ciambrone, M. Gatta, F. Gonnella, and D. Riondino were with the LNF of INFN.

M. Mascolo, R. Messi were with RM-2 Department of INFN, via della Ricerca Scientifica, 1, 00133 Rome, Italy and with the University of Rome “Tor Vergata” – Physics department.

D. Moricciani was with RM-2 Department of INFN.

Using an FPGA-based TDC requires others compromises to be reached, so you need to consider also: how many resources are needed to implement the TDC, how simple is to correct nonlinearities, how simple is to Place And Route (PAR) the circuit in the FPGA lattice, etc. Actually, typical time-requirements for the routing of a standard system are of the order of the clock period (at best 1.8 ns in a Virtex-5) to match the setup/hold time; instead typical requirements to reduce the nonlinearities effects of a TDC are of order of its resolution (from 10 ps up to 1 ns): this makes the implementation of TDCs challenging.

We developed a readout system based on a TDC for the KLOE upgrade (KLOE-2, [2]). This is a particle physics experiment which studies Kaon physics and works with the Double Annular Φ Factory for Nice Experiments (DAΦNE) accelerator which stores and collide e^- and e^+ . For the upgrade we built a new couple of position detectors, the HETs [3], to study the $\gamma\gamma$ physics. These are made of 29 plastic scintillators coupled with 29 photomultipliers; the signals coming from photomultipliers are discriminated and shaped by a custom frontend electronics. We need a readout system able to:

1. measure the arrival time of the discriminated signals;
2. process data;
3. interface with KLOE-2 trigger and acquisition systems.

All these requirements led us to examine various possible TDC architectures and to focus on those which allow us to implement on the same FPGA all the parts we need. Finally we decided for the 4xOversampling [3] technique.

In the work described in this paper we pushed the resolution of the 4xOversampling technique to its limit implementing a TDC using very few FPGA resources. In the next section we will introduce the techniques we used (Nutt interpolation and 4xOversampling) and, for comparison, the Multitapped Delay Line technique that is the most commonly used. Afterwards the characteristics of the TDC will be examined.

II. TDC ARCHITECTURE

A. The Nutt interpolation method

The simplest way to implement a TDC is to use a “coarse counter” that starts counting with the “start” pulse and ends with the “stop” pulse. To improve the resolution of such converter the clock period T_{clk} must be decreased as much as pos-

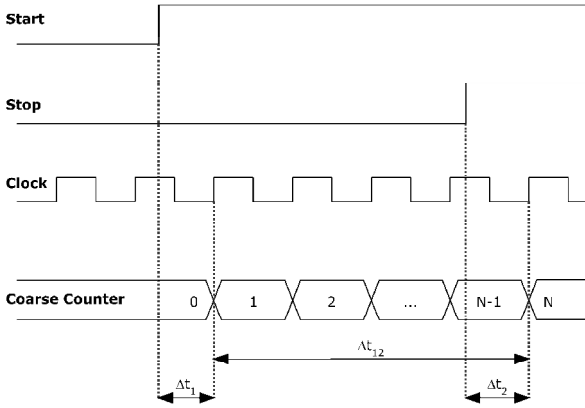


Fig. 1. The Nutt interpolation method.

sible: with a Virtex-5 FPGA this means a max-resolution of about 2 ns.

The method of the counter has a peerless advantage: the almost unlimited range. Increasing the number N_{bit} of the counter bits the range R of the TDC will increase as well:

$$R = 2^{N_{bit}} \cdot T_{clk} \quad (1)$$

This is why the method of the counter is always used in a combination with other techniques that improve its resolution: this is called “Nutt interpolation method” or simply “interpolation method” [5],[6]. The time interval T to be measured is divided into three subintervals (Fig. 1). One interval Δt_{12} (which may be quite long) is measured in real time by a coarse counter; the remaining two short intervals, Δt_1 and Δt_2 (at the beginning and at the end of the interval T), are measured by two (or one) high resolution TDCs that are usually called interpolators. Since the interpolator measures the time between the STOP/START pulse and the next positive edge of the clock, its range has to be just longer than one clock period (typically few ns).

So, the main difference between TDC architectures regards on the interpolator. Since the FPGA can implement only digital circuits, the only interpolator we can use are the digital ones. There are two main families of digital interpolators: the first is based on multitapped delay lines; the second is based on two oscillators with slightly different frequencies. The second approach is, anyway, rarely used because of the dead time during the measurement. Even if the 4xOversampling can be traced back to the multitapped delay line family, we will treat

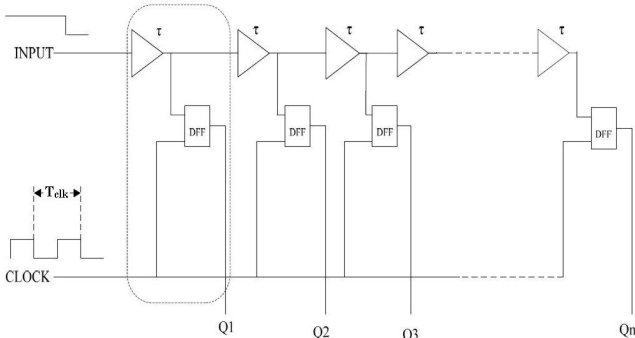
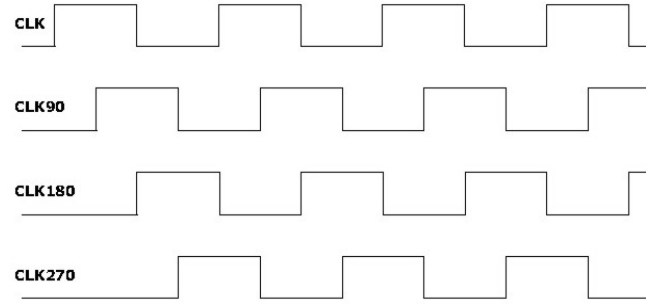
Fig. 2. Multitapped delay line. Each output of the delay line is sampled by one flip-flop: this provides a time resolution equal to τ .

Fig. 3. The four clock signals used to sample the input data.

it as a third method because of its peculiarities.

B. The multitapped delay lines TDC

The most used interpolator architectures are based on the multitapped delay lines and on the multitapped delay lines in Vernier configuration [6],[7]. In these cases the delay lines are fed with the STOP/START pulses and the outputs are sampled by flip-flops at the rising edge of the clock (Fig. 2). Afterwards a decision logic produces a measure of the time between the positive edge of the clock and the input signal.

Since the FPGAs are not designed for TDC implementation, it is not easy to realize a multitapped delay line. Even if you can find embedded delay lines in some FPGAs (Virtex-5 for example) they are not suitable to implement architectures like the one shown in Fig. 2 because they have just one output. Anyway there are other possible solutions. For example the Configurable Logic Blocks (CLBs or Slices in the Virtex FPGAs) have carry-chains for the implementation of adders: these chains are very fast and the delays between two outputs are very small (few hundred of picoseconds), so they can be used as multitapped delay lines. Each interpolator must have a range longer than 1 clock period so the tapped delay line must be at least 1 clock period long. Since the delay time of the carry-chain in one Virtex-5 slice (from the input to the output) is about 100 ps, we need 25 slices to implement a 2.5 ns (400 MHz clock period) delay line. Besides, much additional logic is necessary to implement some algorithms to correct the nonlinearity effects and to improve the resolution [1]. Therefore, if we don't need a very high time resolution, this would be a useless complication and a waste of resources. Similar conclusions are valid also for the others techniques used to implement multitapped delay lines.

C. The 4xOversampling technique

In the 4xOversampling the main clock feeds the Digital Clock Manager (DCM) of the Virtex-5 to generate other 3 clock signals with appropriate phases. In particular, if the clock signal “clk” has period T_{clk} , the DCM provides the following signals (see Fig. 3): “clk90” (delayed by $T_{clk}/4$), “clk180” (delayed by $T_{clk}/2$), “clk270” (delayed by $3T_{clk}/4$). The 4xOversampling technique consists basically on sampling the input signal via 4 flip-flops clocked with each of the 4 signals generated by the DCM (Fig. 4). Such samples feed other flip-flops to be synchronized to the same clock domain, clk,

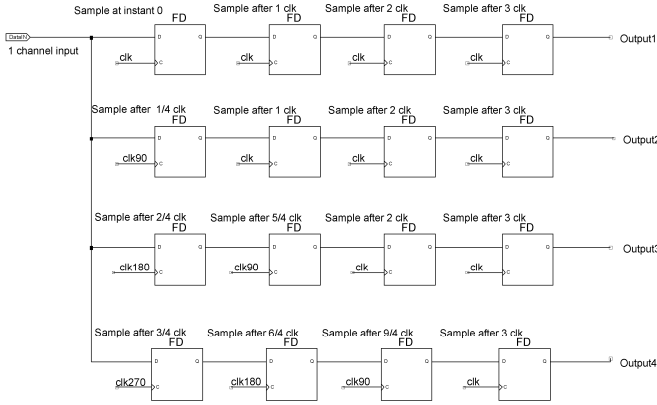


Fig. 4. Input stage of the 4xOversampling technique. The input signal is sampled by the flip-flops of the first column four times each clock period

and avoid metastability. This circuit samples the input signal four times each clock period and, then, a “decision logic” produces a 2-bit measure of the time between the positive edge of the clock signal *clk* and the input signal.

III. 4XOVERSAMPLING FEATURES AND TESTS

A. Resolution and clock frequency

The resolution T_0 (the smallest time interval that can be resolved in a single measure) of the 4xOversampling interpolator is $T_{clk}/4$, so the higher is the clock frequency, the higher is the resolution. In a Virtex-5 FPGA the max clock frequency is 550 MHz but it is very difficult to manage the timing problems of the routing. Therefore we decided to use a 400 MHz clock frequency which corresponds to a 625 ps resolution that is enough for our purpose. In order to minimize timing problems of the routing we divided the system into 2 clock domains: the first at 400 MHz and the second at 100 MHz. The input stage of the TDC (Fig. 4), the decision logic, the coarse counter and a stack memory buffer in which the measures are stored, belong to the first domain. The readout and interface logic, reading the stack buffer when is triggered by the KLOE-2 acquisition system, belongs to the second domain.

The timing problems of routing occur when the setup and hold times are not kept, these are due to two main reasons:

- 1) nets are too long;
- 2) fan-out of the signals is too high.

Pipelines can be used to reduce the length of the nets by properly placing its flip-flops in the FPGA lattice. The fan-out can be reduced by using tree structure along the pipeline. Advanced constraint commands of the synthesis and PAR tools have to be used to place a group of components in a delimited area of the FPGA lattice, to place the flip-flops forward or backward, to duplicate the signals and so on. The matching of the time requirements has been checked through post-PAR simulations or on the timing reports of the PAR tool.

B. Precision and quantization error

In a real TDC the precision σ (the standard deviation of the distribution of repeated measures) is worsened by many con-

tributions (quantization error, clock jitter, input jitter, electronic noise, temperature and power variations, etc.). If the resolution is not very high the most important contribution is the quantization error: this is not avoidable and can be reduced only by increasing the resolution itself. The precision of an ideal TDC (one in which only the quantization worsen the precision) can be evaluated as function of the decimal part c of the ratio T/T_0 [$c = \text{Frc}(T/T_0)$] by means of the following equation [6]:

$$\sigma = T_0 \cdot \sqrt{c(c-1)}. \quad (2)$$

The average value σ_{av} of the precision $\sigma(c)$ can be evaluated by integrating the (2) in the interval $0 \leq c < 1$:

$$\sigma_{av} = \frac{\pi \cdot T_0}{8} \approx 0.393 T_0. \quad (3)$$

The function (2) is plotted (continuous line) in Fig. 5 together with the σ measured for 4xOversampling TDC (asterisks). The σ of the real TDC differs from that of the ideal TDC only on the borders where the effects of the quantization are negligible and other contributions are more evident. The average of the measured σ is $0.408 T_0$ (255ps) and can be compared with that of the ideal TDC (3): the difference is very small (9 ps).

C. Differential nonlinearity

The Differential NonLinearity (DNL) is the deviation of a single quantization step from the ideal value by 1 Last Significant Bit (LSB). One of the most attractive feature of the 4xOversampling technique is the low DNL: actually the quantization step is an integer fraction of the clock period; this is not true in other techniques leading to bigger non-linearity effects.

In the circuit of Fig. 4 the main contributions to the DNL are:

1. the skew of the clock signals;
2. the skew of the input signal;
3. the precision of the DCM to provide 90° shifted clock signals.

While the third point is an intrinsic feature of the FPGA and can't be reduced anymore, something can be done for the others contributions. Since the clock signals are fed through dedicated global nets their skew should be low; anyway we can invert the clock signal inside each slice so only two signals have to be routed and the skew is reduced. The PAR tool of

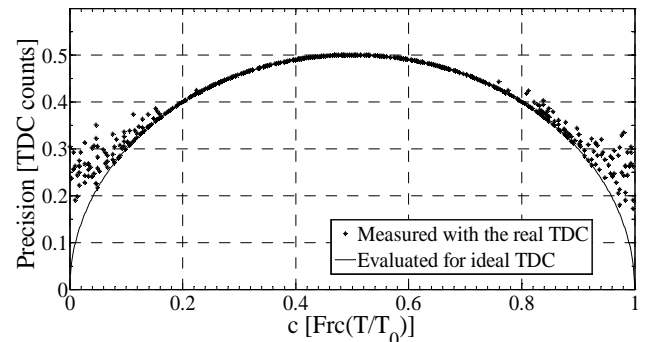


Fig. 5. Precision as function of the decimal part of the ratio T/T_0 .

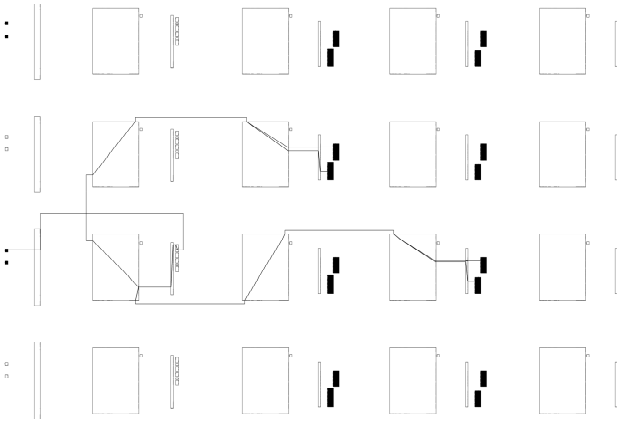


Fig. 6. Routing of the input stage. The small squares on the left are the input pins of the FPGA, the black rectangles are the slices while the bigger blank rectangles are the switch matrixes. The continuous line is the net of the input signal. This routing was chosen by trying to minimize the skew of the net. The neighboring input pins can be used for other input channels of the TDC.

Xilinx provides two constraint commands to limit the skew and the delay of the input signal, but better performances can be obtained by manually placing the input flip-flops. So, trying several placements of these flip-flops in the FPGA lattice, we minimized the skew by checking the PAR reports. For each acceptable placement (Fig. 6) we measured the DNL for a single interpolator (Fig. 7) and for the whole TDC channel (the two interpolators and the coarse counter, Fig. 7). For our final purpose the DNL of the whole TDC is obviously more impor-

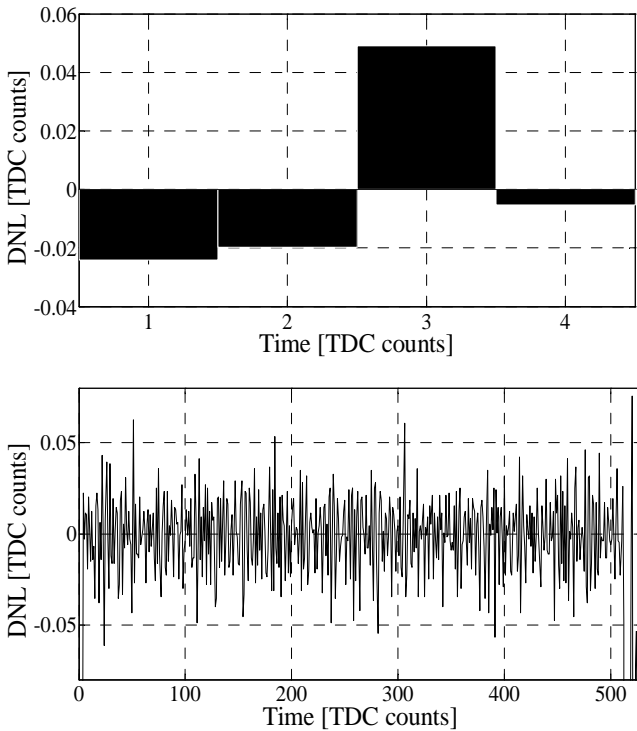


Fig. 7. Differential Nonlinearity of a single interpolator (plot on the top) and for one channel that implements the interpolation technique (plot on the bottom).

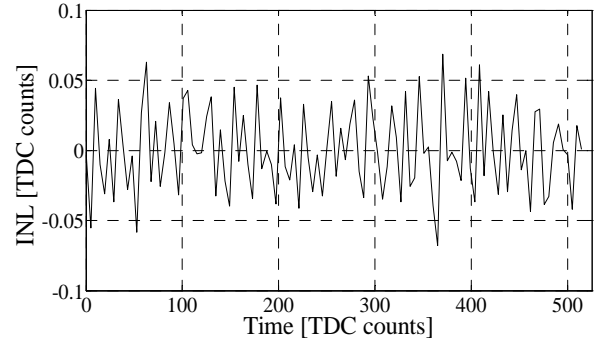


Fig. 8 Integral nonlinearity.

tant than the DNL of a single interpolator. In the second plot of Fig. 7 we can neglect the results for TDC output bigger than 510 counts and smaller than 3 counts because in those ranges the behavior is not due to the TDC but to the readout logic interfering with measurement recording. Nevertheless, for the HET detectors, we will only use the TDC in a range between 30 counts and 465 counts; in this range the DNL_{max} is about 0.05 TDC counts (31.2 ps).

D. Integral nonlinearity

Integral NonLinearity (INL) is the deviation of the input-output characteristic from the ideal straight line. The straight line is obtained by interpolating the measures. Since the TDC is essentially a counter the INL is very small: Fig. 8 shows that the INL_{max} is about 0.05 TDC counts (31.2 ps).

E. Resource utilization

As we pointed out before in this paper, the most attractive feature of the 4xOversampling is the low resources utilization. The final report of the PAR tool can be used to evaluate the resources usage of each module. Table 1 reports the utilization levels of one channel of a 4xOversampling TDC with resolution of 625 ps, range of 640 ns (that corresponds to 10 bits measures) and a memory buffer of 40 bytes (that correspond to 32 consecutive measures). These numbers can be compared with the total number of slices in a Virtex-5 FPGA (44,800 in a FX70T, each slices contains four 6-input LUTs and four flip-flop registers). Nevertheless the slices are often only partially used and they can be employed to implement also other logic modules. Each TDC channel uses one differential couple of pins; Fig. 6 shows that the modularity of the routing allows employing nearby couple of pins to implement other channels.

TABLE I
MODULE LEVEL UTILIZATION

Module name	Used slices	Used slice Registers	Used slice LUTs
Input stage	8	16	8
1 interpolator stage (input stage & decision logic)	16	35	15
Coarse 8-bits counter	5	15	9
Logic for the implementation of the interpolation method	4	11	0
Buffer memory (40 bytes)	69	213	44
Total for 1 channel TDC	94	274	68

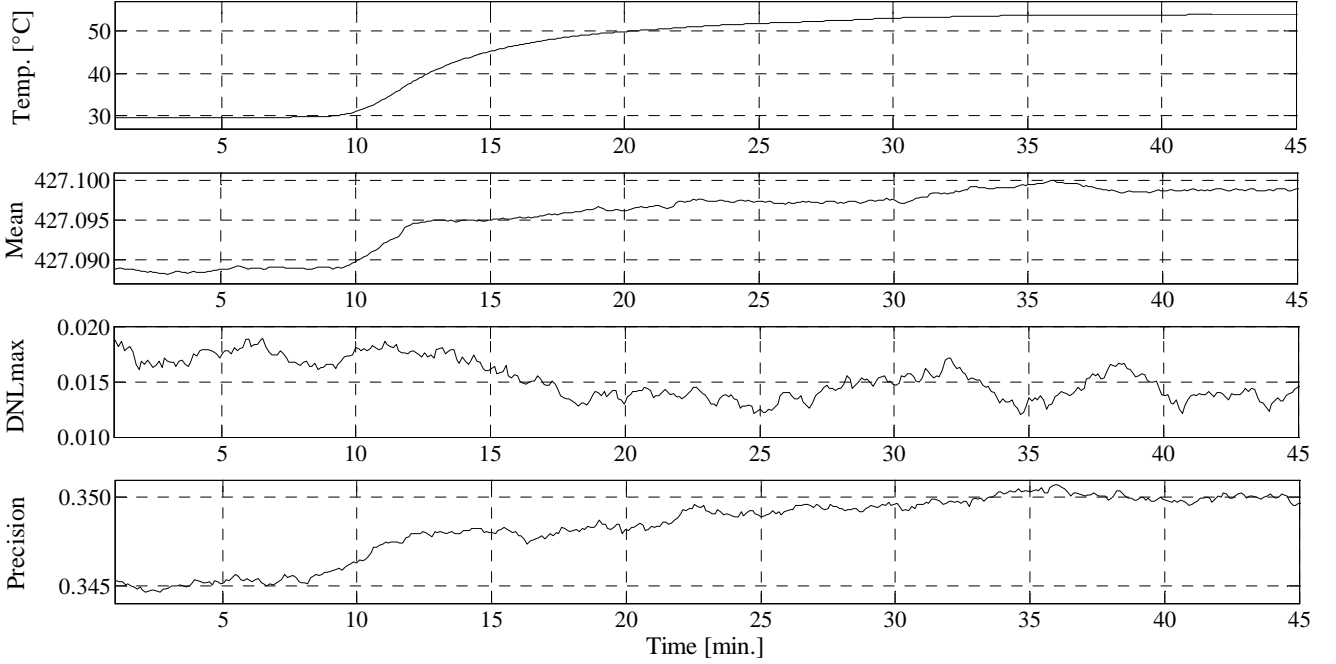


Fig. 9. Temperature effects on the performances of the TDC. The mean value, the precision and the DNL_{max} are measured in TDC counts.

So, we can infer that the 4xOversampling technique allows to maximize the number of channels that can be implemented into a FPGA.

Finally, we can compare the utilization level of the input stage of the 4xOversampling technique with the one of the tapped delay line technique. As we evaluated in section II.B, the sampling stage of the tapped delay line uses at least 25 slices (even more to implement some logic to reduce the DNL) instead of 8 (this includes all the flip-flops in Fig. 4). On top of that, the implementation of channels using contiguous pins could be challenging for the tapped delay lines.

F. Temperature effects

Although we do not expect significant temperature effects on the TDC performances we decided to make an exhaustive test including temperature variations. Performing temperature measurements of the FPGA die is very simple because Virtex-5 has an embedded temperature sensor. In order to change the temperature, we just switched off the cooling system of the FPGA and switched on a heater. In this way, the temperature of the FPGA increases of about 25 °C.

We measured repetitively the same time interval while changing the temperature of the FPGA. The measured interval was chosen with a small value of c (see section III.B) where temperature effects are more evident. In Fig. 9 is shown that the mean value of the measured time interval ($8 \cdot 10^5$ samples) changes with the temperature of about $4 \cdot 10^{-4}$ TDC counts/°C (0.25 ps/°C). Also the precision changes of about $2 \cdot 10^{-4}$ TDC counts/°C (0.12 ps/°C) while the DNL_{max} changes less than 10^{-4} TDC counts/°C (0.06 ps/°C).

IV. TDC AND DATA ACQUISITION FOR HET TAGGERS

A. The 4xOversampling technique to distinguish the bunches of DAΦNE

We applied the 4xOversampling technique to the data ac-

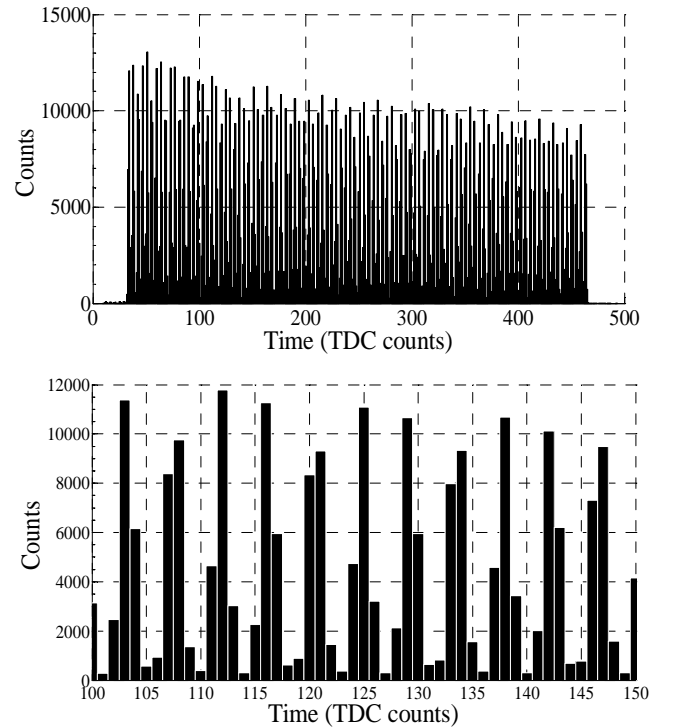


Fig. 10. Histograms of the time measures performed with the TDC fed by the HET detector installed on DAΦNE. The second plot is a detail of the first; they both show the bunch structure of the beam.

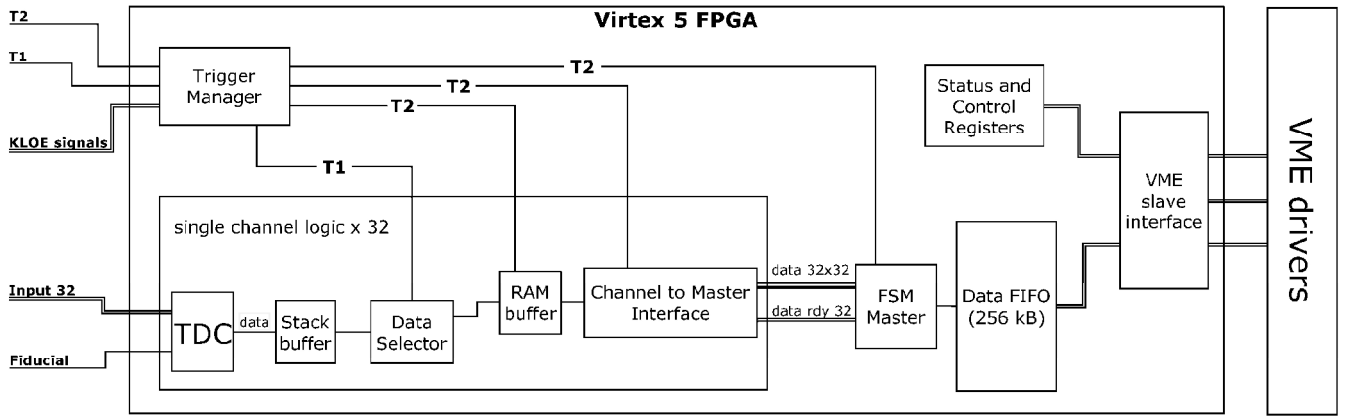


Fig. 11. Simplified scheme of the TDC and of the readout system of the HET. Some logic elements are replicated for each channel of the TDC. KLOE-2 DAQ system provides the triggers and some other control signals.

quisition of the HET particle detectors. In order to reconstruct the physics events we need to associate each detected particle to the right bunch crossing at the KLOE-2 IP. The beam of DAΦNE has a 120 bunches structure of which only the first 100 contain particles; the time separation between two consecutive bunches is 2.7 ns.

The association can be done by measuring the time between a signal provided by the machine (Fiducial) that identifies the first bunch, and the instant on which the particle has been detected.

Fig. 10 shows the bunch structure of the beam deduced by repeated TDC measures of the signals from the HET detectors. This plot can be used both for the calibration of the TDC and for association of the detected particles to the proper bunch; it also shows that the TDC has enough resolution to accomplish its task.

B. The readout system of the HET detectors

Thanks to the few resources used by the 4xOversampling technique, we were able to implement a complete DAQ system on a Virtex-5 FPGA comprehensive of a 32 TDC channels.

The TDC performs measurements continuously, producing a big amount of data but only a small fraction contains valid information. In order to select and store only relevant data, the KLOE trigger signals T1 and T2 are exploited and a zero suppression algorithm is implemented to discard all the useless data. In Fig. 11 a simplified scheme of the whole acquisition system is represented. The data are stored, moved and selected through three buffer stages (Stack Buffer, RAM buffer, Data FIFO) by three Finite State Machines (Data Selector, Channel to Master Interface, FSM Master). The first buffer stage of the DAQ (Stack memory) assures to read out only the most recent data; this is done by writing a peculiar word (Fiducial Tag) just before the first bunch, in order to recognize the most recent cycles. The latest FSMs and buffers implement the zero suppression algorithm and manage the trigger signals from KLOE-2. The content of the main buffer (Data FIFO) can be accessed via a A32/D64 VME64x interface.

In order to test and monitor the HET DAQ we also imple-

mented some facilities for debugging and a scaler (not shown in Fig. 11) used to measure the detector rates.

So, we developed a general purpose VME board that hosts a FX70T Virtex-5 FPGA for the readout of the HET detectors. This board has 32 differential inputs for the TDC, an embedded DDR2 RAM memory for long data storage and many interfaces (VME, Ethernet, USB, RS232, Optical links) for readout, monitoring and debug.

V. CONCLUSION

In these last years several works were published about the implementation of TDCs on FPGAs. Such works usually are aimed to improve the resolution and often do not care about the possibility of implementing a big number of channels along with embedded acquisition systems on the same device.

With this work we showed how to implement a TDC with very low resources occupancy, a negligible dead time (multi-hit), reduced DNL and long range. Even if the resolution is big in comparison to the other architectures, this approach has a lot of applications, out of which we showed the example of KLOE-2 $\gamma\gamma$ tagging system.

Future studies will aim to improve the resolution while keeping the FPGA resource utilization level at minimum; the Vernier technique, which uses two oscillators with slightly different periods, seems very promising [8].

REFERENCES

- [1] Wu, Jinyuan and Shi, Zonghan, "The 10-ps wave union TDC: Improving FPGA TDC resolution beyond its cell delay," *Nuclear Science Symposium Conference Record*, 2008. NSS '08. IEEE, pp. 3440 – 3446, February 2009.
- [2] G. Amelino-Camelia et al., "Physics with the KLOE-2 experiment at the upgraded DAΦNE," *EPJC*, 68 (2010), pp. 619–681, 2010.
- [3] F. Archilli, et al., "The high energy tagger for gamma gamma physics at KLOE2," *Nucl.Instr.AndMeth.A2009*, doi:10.1016/j.nima.2009.06.082.
- [4] N. Sawyer, "Data to Clock Phase Alignment, XApp225," *Xilinx Application Note*, Xilinx, February 2009.
- [5] R. Nutt, "Digital time intervalometer," *Rev. Sci. Instrum.*, vol. 39, pp. 1342-1345, 1968.

- [6] J. Kalisz, "Review of methods for time interval measurements with picoseconds resolution," *Metrologia*, vol.41, pp. 17-32, 2004.
- [7] J. Kalisz, R. Szplet, and A. Poniecki, "Field programmable gate array-based time-to-digital converter with 200-ps resolution," *IEEE Trans. Instrum. Meas.*, vol. 46, no. 1, pp. 51-55, Feb. 1997.
- [8] M. Lin, G. Tsai, C. Liu, S. Chu, "FPGA-based high area efficient time to digital IP design," *TENCON 2006. 2006 IEEE Region 10 Conference*, pp. 1-4, Nov. 2006.